Synthesis and Thermal Behavior of Crystalline Hydrated Iron(III) Phosphates of Interest as Positive Electrodes in Li Batteries

Priscilla Reale and Bruno Scrosati

Dipartimento di Chimica, Universita La Sapienza, 00185 Roma, Italy

Charles Delacourt, Calin Wurm, Mathieu Morcrette, and Christian Masquelier*

Laboratoire de Réactivité et Chimie des Solides, Université de Picardie Jules Verne, 33 Rue St. Leu, 80039 Amiens Cedex 9, France

Received August 1, 2003

Four different hydrated iron phosphates were prepared as pure crystalline powders by precipitation in aqueous solutions under controlled pH: strengite, $FePO_4 \cdot 2H_2O$ (*Pbca*; a = 9.8923(6) Å, b = 10.125(1) Å, c = 8.729(1) Å); metastrengite I, $FePO_4 \cdot 2H_2O$ (*Pbnm*; a = 5.226(2) Å, b = 10.026(3) Å, c = 8.917(3) Å); metastrengite II, $FePO_4 \cdot 2H_2O$ ($P2_1/n$; a = 5.3276-(3) Å, b = 9.800(1) Å, c = 8.7129(6) Å, β = 90.532(6)°); and spheniscidite, $NH_4(Fe_2(PO_4)_2\text{-}OH \cdot H_2O) \cdot H_2O$ ($P2_1/n$; a = 9.808(3) Å, b = 9.727(3) Å, c = 9.866(3) Å, β = 102.85(2)°). Thermogravimetric analysis revealed slightly more than 2 H_2O molecules per $FePO_4$ for the first three compounds, the excess being considered as adsorbed on the powders' surface. Temperature-controlled X-ray diffraction allowed isolation and determination of the stability domains of a large number of $FePO_4$ polymorphs which may, or may not, reabsorb H_2O upon exposure to ambient air. All these phases, after careful optimization of the electrode preparation, may be reversibly reduced to ∼90% of their theoretical capacities within the 2−4 V vs Li^+/Li region.

1. Introduction

Lithium iron phosphates have recently become the object of great interest in the field of positive electrode materials for lithium batteries.[1] The olivine $LiFePO_4$[2−3] is without doubt an appealing electrode material thanks to its two-phase deinsertion−insertion process at 3.45 V vs Li^+/Li. The main drawbacks in the choice of $LiFePO_4$ are related to its poor intrinsic electronic and ionic conductivities, its small tap density,[4] and the fact that iron is in the +2 oxidation state, which requires very careful synthetic procedures to prevent the formation of stable Fe(III) phosphates. At present, and following the work of Armand's group,[5−6] several research groups have focused on improving the overall performances of $LiFePO_4$ through the optimization of the size of the particles[7] that are subsequently coated with conductive carbon.[8]

Other groups have focused on the synthesis and electrochemical evaluation of Fe^{3+}-containing iron phosphates, i.e., compositions prone to reduction to Fe^{2+} through reaction with lithium.[9−19] For instance, Prosini,[17] Hong,[18] and Croce[14] reported on Li insertion into the crystalline α form of $FePO_4$ quartz. Additionally, it was shown that amorphous hydrated $FePO_4 \cdot nH_2O$ undergo surprisingly reversible and stable redox reactions at an average voltage of ∼3 V vs Li^+/Li corresponding to reduction of almost all of Fe^{3+} into Fe^{2+}.[12,18,19]

* To whom correspondence should be addressed. E-mail: christian.masquelier@sc.u-picardie.fr.

(1) Padhi, A. K.; Nanjundaswamy, K. S.; Masquelier, C.; Okada, S.; Goodenough, J. B. *J. Electrochem. Soc.* **1997**, *144* (5), 1609−1613.
(2) Padhi, A. K.; Nanjundaswamy, K. S.; Goodenough, J. B. *J. Electrochem. Soc.* **1997**, *144*, 1188.
(3) Goodenough, J. B.; Padhi, A. K.; Nanjundaswamy, K. S.; Masquelier, C. U.S. Patent 5,910,382, 1997; U.S. Patent 6,391,493 B1, 2002.
(4) Chen, Z.; Dahn, J. R. *J. Electrochem. Soc.* **2002**, *149* (9), A1184−A1189.
(5) Ravet, N.; Goodenough, J. B.; Besner, S.; Gauthier, M.; Armand, M. *Proceedings of the 196th Electrochemical Society Meeting*, Vol. 99-2, Oct. 1999; Electrochmical Society, Inc.: Pennington, NJ; 1999.
(6) Armand, M.; Gauthier, M.; Magnan, J. F.; Ravet, N. WO Patent 02/27823, 2002.
(7) Yamada, A.; Chung, S. C.; Hinokuma, K. *J. Electrochem. Soc.* **2001**, *148* (3), A224−A229.
(8) Huang, H.; Yin, S. C.; Nazar, L. F. *Electrochem. Solid State Lett.* **2001**, *4* (10), A170−A172.
(9) Masquelier, C.; Padhi, A. K.; Nanjundaswamy, K. S.; Goodenough, J. B. *J. Solid State Chem.* **1998**, *135*, 228−234.
(10) Andersson, A. S.; Kalska, B.; Eyob, P.; Aernout, D.; Häggström, L.; Thomas, J. O. *Solid State Ionics* **2001**, *140*, 63.
(11) Eyob, P.; Andersson, A. S.; Thomas, J. O. *J. Mater. Chem.* **2002**, *12*, 1−6.
(12) Song, Y.; Yang, S.; Zavalij, P. Y.; Whittingham, M. S. *Mater. Res. Bull.* **2002**, *37*, 1249−1257. Song, Y.; Yang, S.; Zavalij, P. Y.; Whittingham, M. S. *Electrochem. Commun.* **2002**, *4* (2), 239−244.
(13) Song, Y.; Zavalij, P. Y.; Suzuki, M.; Whittingham, M. S. *Inorg. Chem.* **2002**, *41* (22), 5778−5786.
(14) Croce, F.; D'Epifanio, A.; Reale, P.; Settimi, L.; Scrosati, B. *J. Electrochem. Soc.* **2003**, *150* (5), A576−A581.
(15) Morcrette, M.; Wurm, C.; Masquelier, C. *Solid State Sci.* **2002**, *4*, 239−246.
(16) Wurm, C.; Morcrette, M.; Rousse, G.; Dupont, L.; Masquelier, C. *Chem. Mater.* **2002**, *14*, 2701−2710.
(17) Prosini, P. P.; Lisi, M.; Scaccia, S.; Carewska, M.; Cardellini, F.; Pasquali, M. *J. Electrochem. Soc.* **2002**, *149* (3), A297−A301.
(18) Hong, Y. S.; Ryu, K. S.; Park, Y. J.; Kim, M. G.; Lee, J. M.; Chang, S. H. *J. Mater. Chem.* **2002**, *12*, 1870−1874.
(19) Masquelier, C.; Reale, P.; Morcrette, M.; Wurm, C.; Dupont, L.; Larcher, D. *J. Electrochem. Soc.* **2002**, *149* (8), 1−0.

10.1021/cm031107z CCC: $25.00
Published on Web 12/04/2003

The beneficial role of the inductive effect exercised by the polyanion has been evidenced once again, as the value of the Fe^{3+}/Fe^{2+} redox couple has been measured at 3.2 V vs Li^+/Li for $Li_xFe_4(P_2O_7)_3 \cdot nH_2O$, whereas it was only at 3.0 V vs Li^+/Li for $Li_xFePO_4 \cdot nH_2O$, as a consequence of the different local environments around Fe atoms.[19] Interestingly, "H_2O" groups appeared to be unreactive in this potential domain and promote higher ionic conductivity.

In this work we go deeper into the understanding of the synthesis conditions and the thermal behavior of several crystalline hydrated iron phosphate allotropes. During the course of our study, Whittingham's group communicated a detailed comparative structural study of two crystalline phases of $FePO_4 \cdot 2H_2O$ (orthorhombic strengite and monoclinic phosphosiderite, labeled as metastrengite II throughout this paper) synthesized hydrothermally as single crystals, which, under vacuum at 353 K, transformed to orthorhombic and monoclinic forms of $FePO_4$, respectively.[13] However, as far as electrochemistry is concerned, the hydrothermal procedure described by Song has the disadvantage of producing mixtures of several iron phosphates with high crystallinity.

We adopted a "wet chemistry" route to prepare pure strengite and metastrengite II powders and a third $FePO_4 \cdot 2H_2O$ crystalline allotrope, labeled as metastrengite I.[20−22] The spheniscidite $NH_4(Fe_2(PO_4)_2OH \cdot H_2O) \cdot H_2O$ was also obtained under specific pH conditions. In this paper, we examined in much detail the thermal behavior of all four of these phases through thermogravimetric analysis and temperature-controlled X-ray diffraction, which allowed us to enlight the existence of a very wide variety of intermediate $FePO_4$ phases. The hydrated materials were tested as positive electrodes in lithium secondary cells. Electrodes optimization was particularly important for reaching reasonable electrochemical response, this stressing again the relevance of morphology and electronic contacts between iron phosphate particles.

2. Experimental Section

Hydrated iron(III) phosphates were synthesized by a wet chemistry method consisting of allowing the nucleation and growth of crystalline products in dilute water solutions. The detailed procedures for each of the phases investigated will be given later on in the appropriate sections of this paper. The powders' morphology was observed by scanning electron microscopy (FEG XL-30) and the specific surface calculations were carried out by means of physisorption of N_2 at 77 K and BET calculations. Thermal analysis was performed by means of a Setaram TG-DTA 92-B apparatus, with heating rates of 5 °C/min under air between 298 and 1073 K.

X-ray powder diffraction measurements were performed using either a Philips PW 1710 diffractometer (Cu Kα radiation, back monochromator) or a Bruker D8 diffractometer (Co Kα radiation, PSD counter) equipped with an Anton Parr Chamber HTK 1200 °C. For the temperature-controlled X-ray diffraction study, a pattern was recorded (∼15 min) at constant temperature intervals of 10 °C between which the powder was heated at a rate of 3 °C/min. The powder diffraction diagrams were evaluated using the Fullprof package.[23]

Electrochemical characterization was carried out through galvanostatic techniques in terms of charge−discharge potential profiles, using a VMP or a MacPile automatic cycling/data recording system (Biologic SA, Claix, France). Swagelok type cells were assembled in an environmentally controlled drybox. The negative electrode was a disk of lithium metal foil. A Whatman GF/D borosilicate glass fiber sheet, soaked in a 1 M solution of $LiPF_6$ in EC/DMC (1:1), was placed between the two electrodes. The composite positive electrodes contained 16.7 wt % of acetylene black and 83.3 wt % of active material. Intimate mixing was ensured by ball-milling for 90 or 120 min.

3. Synthesis of Crystalline Hydrated Iron Phosphates

In a previous work,[19] we indicated that amorphous $FePO_4 \cdot nH_2O$ compositions can be precipitated by raising the pH (up to 7−8) of any aqueous solution containing Fe^{3+} and PO_4^{3-} ions. To our knowledge, there is still only limited literature on the thermodynamics and kinetics of phase formations in the $Fe_2O_3-P_2O_5-H_2O$ system. More than 30 years ago though, Rémy, by analogy with d'Yvoire's work on $AlPO_4 \cdot 2H_2O$ varieties,[20] reported for the first time the existence of three allotropes of $FePO_4 \cdot 2H_2O$: strengite, metastrengite II, and metastrengite I, which led, each upon dehydration, to a complicated series of phase transformations before transforming at high temperature (∼1000 K) to $FePO_4$ quartz.[21−22]

Following Rémy's results, and contrary to Song's recent contributions,[12−13] we have synthesized pure microcrystalline powders of the three allotropes (strengite, metastrengite I, and metastrengite II) of $FePO_4 \cdot 2H_2O$. These three phases were precipitated from aqueous solutions of H_3PO_4 (0.027 M) and $FeCl_3 \cdot 6H_2O$ (0.009M), with a careful control of pH being necessary to obtain each allotrope with a high purity. Indeed, the value of the pH has a great influence upon the kinetics of the precipitation reactions. Reaction time appeared to be of great importance as the precipitated phase tends to turn into the more stable one (metastrengite II). When NH_3 is used as an agent for raising the pH of the solution, crystallization of pure and well-crystallized spheniscidite $NH_4(Fe_2(PO_4)_2OH \cdot H_2O) \cdot H_2O$ occurs. The syntheses were carried out in a refluxing apparatus at boiling temperature, under continuous stirring to avoid agglomeration of the particles. All the precipitates were filtered, washed first with distilled water and acetone, and finally dried at a mild temperature (55 °C). Table 1 gathers the more suitable and reproducible synthetic conditions for the obtention of each of the four phases investigated.

3.1 Strengite $FePO_4 \cdot 2H_2O$. Strengite is the orthorhombic (*Pbca*) allotrope of $FePO_4 \cdot 2H_2O$, and belongs to the wide variety of variscite isotypic series: $AlPO_4 \cdot 2H_2O$ (variscite),[24] $FeAsO_4 \cdot 2H_2O$ (scorodite), $InPO_4 \cdot 2H_2O$, etc. $FePO_4 \cdot 2H_2O$ strengite was obtained by precipitation from a dilute solution, when the pH was raised to around 3 by addition of NaOH. This hydroxide was preferred to NH_3, because the latter was found to participate in the precipitation reaction of spheniscidite (see section 3.4). After 2 days of aging under boiling conditions, a fine and well-crystallized yellowish powder

(20) d'Yvoire, F. *Bull. Soc. Chim. Fr.* **1961**, *372*, 1762−1776.
(21) Rémy, P. PhD Thesis, Université de Paris 1971.
(22) Rémy, P.; Boullé, A. *C. R. Acad. Sci.* **1961**, *253*, 2699.
(23) Rodríguez-Carvajal, J. *J. Phys. B* **1993**, *192*, 55.
(24) Kneip, R.; Mootz, D.; Vegas, A. *Acta Crystallogr.* **1977**, *B33*, 263−265.

Table 1. Synthesis Conditions of Strengite, Metastrengite I and II, and Sphenisidite

	reagents		pH	temp.	reaction time/d
strengite	$FeCl_3 \cdot 6H_2O$ 0.009 M H_3PO_4 0.027 M	NaOH 0.04 M	3−4	refluxing conditions	2
metastrengite I	$FeCl_3 \cdot 6H_2O$ 0.009 M H_3PO_4 0.027 M	xxx	1−2	refluxing conditions	7
metastrengite II or phosphosiderite	$FeCl_3 \cdot 6H_2O$ 0.009 M H_3PO_4 0.027 M	HCl 0.5 M	0−1	refluxing conditions	12
spheniscidite a	$Fe_2(SO_4)_3 \cdot 6H_2O$ 0.5 M $NH_4H_2PO_4$ 1 M	NH_3	∼6	RT	3
spheniscidite b	$Fe_2(SO_4)_3 \cdot 6H_2O$ 0.25 M $NH_4H_2PO_4$ 0.5 M	NH_3	∼6	80 °C	1

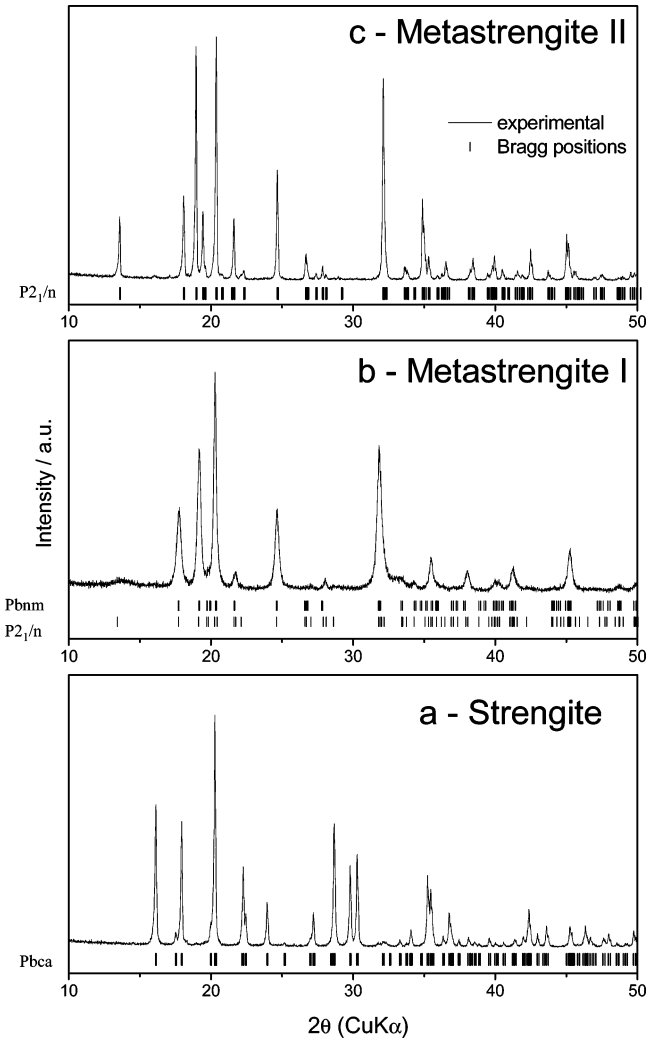

Figure 1. X-ray powder diffraction patterns (Cu Kα radiation) of strengite (a), metastrengite I (b), and metastrengite II (c) $FePO_4 \cdot 2H_2O$, collected for 12 h.

was obtained. The X-ray diffraction pattern of Figure 1a was fully indexed in the orthorhombic space group *Pbca* with lattice parameters that agree well with those reported by Whittingham et al.:[13] $a = 9.892(1)$ Å, $b = 10.125(1)$ Å, and $c = 8.729(1)$ Å. Thermogravimetric analysis (Figure 2) indicated a total amount of 2.1 H_2O groups per $FePO_4$ unit, i.e., slightly more than the expected stoichiometric amount. This extra amount of 0.1 H_2O was attributed to water adsorption on the particles' surface. Scanning electron micrographs reveal a roughly average particle dimension of 2 μm with a specific surface development of ∼3 m^2/g. Importantly, we noticed that reaction times longer than 2 days led systematically to the progressive appearance of a second

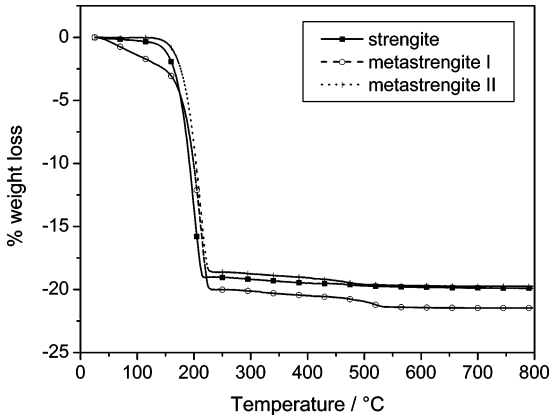

Figure 2. Thermogravimetric analysis of crystalline iron orthophosphates. Heating rate: 5 °C/min from 25 to 800 °C.

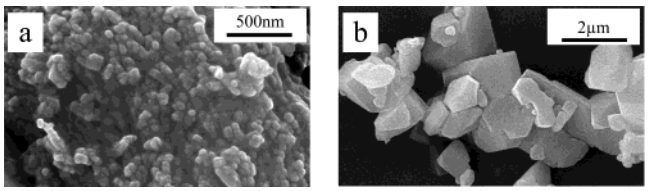

Figure 3. Scanning electron micrograph of as-synthesized metastrengite I (a) and metastrengite II (b) $FePO_4 \cdot 2H_2O$ powders. Magnification: 40 000× (a) and 10 000× (b).

phase, $FePO_4 \cdot 2H_2O$ metastrengite I, together with $FePO_4 \cdot 2H_2O$ strengite.

3.2 Metastrengite I. The crystallization of metastrengite I[21] is favored by more acidic conditions than for strengite. This form of $FePO_4 \cdot 2H_2O$ slowly transforms to metastrengite II after a period of time that depends on the exact initial pH value: it is quicker when the initial value of pH is small. Typically, no acid or basic reactants addition was done because the initial acidic pH value imposed by H_3PO_4 is convenient. To our knowledge, there are no crystallographic data on metastrengite I in the literature. Nevertheless, metastrengite I may be regarded as an intermediate phase between strengite and metastrengite II. This is supported by the pioneering work of d'Yvoire[20] on metavariscite I, a poorly crystalline modification of $AlPO_4 \cdot 2H_2O$, sort of intermediate phase between the two well-known allotropes variscite and metavariscite of $AlPO_4 \cdot 2H_2O$.

For pH values around 1−2, metastrengite I was obtained as a pure microcrystalline powder after one week of reflux. This intermediate form of $FePO_4 \cdot 2H_2O$ is of much smaller crystallite size than strengite as shown by the peak width of the diffraction pattern of Figure 1b. Additionally, SEM micrographs (Figure 3a) indicate that metastrengite I particles are much smaller

than those of strengite. This was further supported by the high specific surface area found by BET calculations, close to 31 m^2/g. Interestingly, such a high surface development seems to have an impact on the amount of "adsorbed" H_2O molecules at the surface of $FePO_4 \cdot 2H_2O$. The thermogravimetric data of Figure 2 shows indeed first a continuous weight loss from room temperature to ~150 °C (~0.3 H_2O per formula unit) and then a more abrupt loss from ~150 to ~220 °C (~2 H_2O per formula unit). The XRD pattern of Figure 1b was indexed either in the monoclinic space group $P2_1/n$ (β = 90.55(1)°) or in the orthorhombic space group $Pbnm$. Of these two possibilities, only the space group $P2_1/n$ may account for the presence of a wide diffraction peak at $2\theta \sim 13°$. However, we noticed that the intensity of this diffraction peak could vary significantly from one batch to another, our interpretation being that it is more likely due to the presence of a small amount of metastrengite II as impurity. As a result, the lattice is more likely to be orthorhombic and was indexed with a = 5.226(2) Å, b = 10.026(3) Å, and c = 8.917(3) Å.

3.3 Metastrengite II. Metastrengite II is isotypic with metavariscite ($AlPO_4 \cdot 2H_2O$), a monoclinic ($P2_1/n$) three-dimensional network differing from the orthorhombic one of variscite by the orientations of the $FeO_4(OH_2)_2$ octahedra and PO_4 tetrahedra.[25] Metastrengite II was obtained pure when an excess of HCl had been added to the initial Fe(III) and phosphate aqueous solution. A very long crystallization time was necessary (12 d) to avoid the presence of impurities of the 2 other allotropes. Under these conditions, metastrengite II appears as pinky platelike crystals of an average dimension of 1−2 μm (Figure 3b), with a surface development estimated to ~2m^2/g. Note that for this compound, obtained at low pH, the precipitation yield was very low; this may be easily understood by plotting the solubility diagram of the Fe(III)/phosphate/H_2O system.[26] Thermogravimetric analysis (Figure 2) indicated a water content corresponding to the stoichiometry $FePO_4 \cdot 2.1H_2O$. The XRD pattern of metastrengite II (Figure 1c) was fully indexed in the monoclinic space group $P2_1/n$ with lattice parameters: a = 5.3276(3) Å, b = 9.800(1) Å, c = 8.7129(6) Å, and β = 90.53(1)°.

3.4 Spheniscidite. Spheniscidite $NH_4(Fe_2(PO_4)_2OH \cdot H_2O) \cdot H_2O$ is a mineral which crytallizes in the moniclinic space group $P2_1/n$. Single crystals were obtained from hydrothermal conditions by Ferey's group who determined the crystal structure.[27] Iron occupies two distinct 6-fold crystallographic sites and the structure is built on "octamers" of 4 FeO_6 octahedra and 4 PO_4 tetrahedra. The formulation $[Fe_4(PO_4)_4(OH)_2 \cdot (H_2O)_2] \cdot (NH_4)_2 \cdot 2H_2O$ describes better the specificities of the structural arrangement and in particular the fact that there are two types of "H_2O" groups in this structure: two of them belong to the $Fe(1)O_6$ octahedra, the two others being "free" and close to NH_4^+ within the eight-membered tunnels of the structure. Within the octamers, two $Fe(2)O_6$ octahedra share an edge through two O(7) equivalent positions to which the hydrogens of the (OH) groups are also linked. Consequently, the Fe−O(7) bonds are much weakened as witnessed by the abnormally long Fe−O(7) bonds of ~2.16 Å.[27]

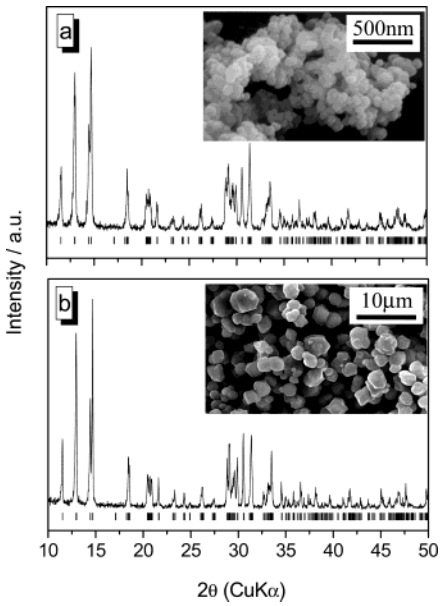

Figure 4. X-ray powder diffraction patterns (Cu Kα radiation) and scanning electron micrographs (50 000× and 2500×) of $NH_4(Fe_2(PO_4)_2OH \cdot H_2O) \cdot H_2O$ powders synthesized at RT from (a) a 1 M solution of Fe(III) and phosphate and (b) at 80 °C from a 0.5 M solution.

We obtained pure microcrystalline powders of $NH_4(Fe_2(PO_4)_2OH \cdot H_2O) \cdot H_2O$ by crystallization in an aqueous solution of $NH_4H_2PO_4$ and $Fe_2(SO_4)_3 \cdot 6H_2O$ in the atomic ratio Fe/P = 1:1, at a pH raised to 6 by addition of NH_3. Depending on the temperature, on the concentration of the precursors, and on the aging time, significant alterations in the morphology of the final product occurred. Figure 4 shows the XRD patterns and the scanning electron micrographs of two samples, synthesized (a) at room temperature from a 1 M solution of Fe(III) and phosphate and (b) at 80 °C from a 0.5 M solution. Both samples are pure crystalline spheniscidite with lattice parameters in excellent agreement with the literature,[27] i.e.: a = 9.808(3) Å, b = 9.727(3) Å, c = 9.866(3) Å, and β = 102.85(2)° in the space group $P2_1/n$. Sample "a" is built on large agglomerates (10−20 μm) of very small particles (average dimension of 100 nm) with a specific surface of 21 m^2/g. Sample "b" is built on big particles of micrometric size and develops a surface area smaller than 1m^2/g. As shown by the XRD patterns though, both samples are very similar in terms of crystallinity.

4. Thermal Behavior

The thermal behavior under air of the four phases described above, still poorly documented in the literature, was investigated with the aim of isolating new iron phosphates intermediates as candidates for the reversible insertion of lithium. As mentioned in the previous section, thermogravimetric analysis indicated various amounts of H_2O per $FePO_4$ within the three cystalline phases strengite, metastrengite I, and metastrengite II. A whole series of temperature-controlled X-ray diffraction experiments are presented here. The procedures consisted of heating rates of 3°C/min between isotherm periods of 15 min every 10 °C, during which the XRD

(25) Kneip, R.; Mootz, D. *Acta Crystallogr.* **1973**, *B29*, 2292−2294.
(26) Delacourt, C. et al. *Proceedings of the 2nd LiBD Meeting, Arachon, France, September, 2003.*
(27) Cavellec, M.; Riou, D.; Férey, G. *Acta Crystallogr.* **1994**, *C50*, 1379−1381.

Table 2. Crystallographic Data of the Synthesized Phases

	formula	space group	*a*/Å	*b*/Å	*c*/Å	*β*/°	BET/m^2/g
strengite	$FePO_4{\cdot}2.1H_2O$	*Pbca*	9.8923(6)	10.125(1)	8.729(1)		2.6
metastrengite I	$FePO_4{\cdot}2.3H_2O$	*Pbnm*	5.226(2)	10.026(3)	8.917(3)		31
metastrengite II or phosphosiderite	$FePO_4{\cdot}2.1H_2O$	$P2_1/n$	5.3276(3)	9.800(1)	8.7129(6)	90.532(6)	2
spheniscidite a	$NH_4(Fe_2(PO_4)_2OH{\cdot}H_2O){\cdot}1.3H_2O$	$P2_1/n$	9.808(3)	9.727(3)	9.866(3)	102.85(2)	21
spheniscidite b	$NH_4(Fe_2(PO_4)_2OH{\cdot}H_2O){\cdot}1.3H_2O$	$P2_1/n$	9.809(2)	9.727(2)	9.863(2)	102.82(1)	<1

Table 3. Thermal Stability Ranges of the Phases Obtained by Annealing of the Crystalline Iron Orthophosphates[a]

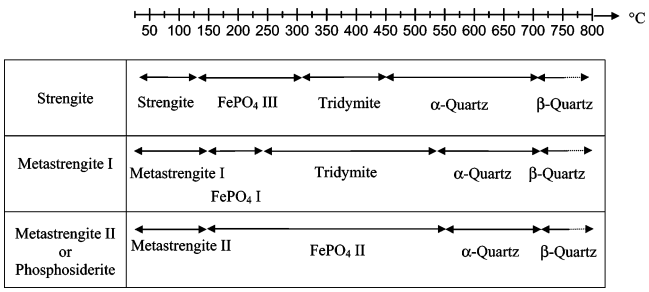

[a] The temperatures given are those at which the new phase (not necessarily pure) begins to form on heating.

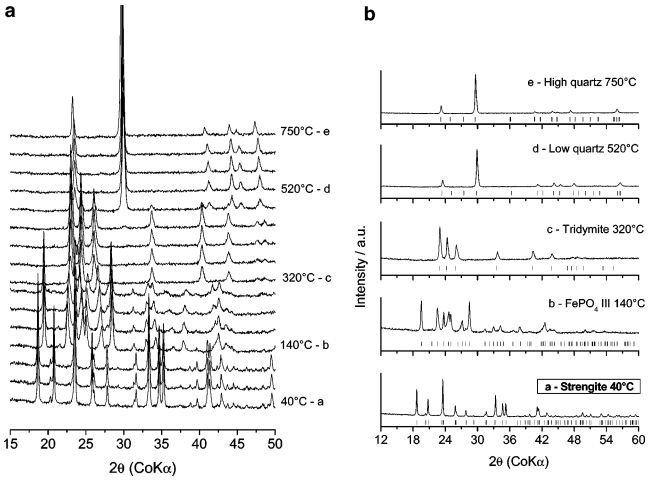

Figure 5. (a) XRD diffraction patterns evolution of $FePO_4{\cdot}2H_2O$ strengite under thermal treatment. Annealing steps of 30 °C at a rate of 3 °C/min followed by collection of diffractograms for 15 min; Co Kα radiation. (b) Details of the XRD patterns of the pure phases produced by annealing of strengite; Co Kα radiation.

patterns were collected. As gathered in Table 3, each of the four pristine compositions behaves in a very distinct manner, even though the final product at high temperature is always the same: $FePO_4$−quartz.

4.1 Strengite $FePO_4{\cdot}2H_2O$. As the temperature is slowly raised, the XRD patterns of pristine strengite $FePO_4{\cdot}2H_2O$ do not evolve until $T \approx 130$ °C (Figure 5), after which constitutional H_2O groups suddenly depart from the structure (Figure 2). This leads to a new form of $FePO_4$ at 140 °C that we will refer to as $FePO_4$ III, consistent with Rémy's notation.[21−22] In the course of our study, Whittingham's group isolated single crystals of this orthorhombic form of $FePO_4$[13] and determined the crystal structure. Dehydration involves in this case only minor rearrangements of the framework even though the Fe−O coordination is reduced from 6 to 4 as a result of the departure of 2 H_2O groups that were directly linked to a given iron. This departure leads to an overall unit-cell shrinkage of 13%, in agreement with

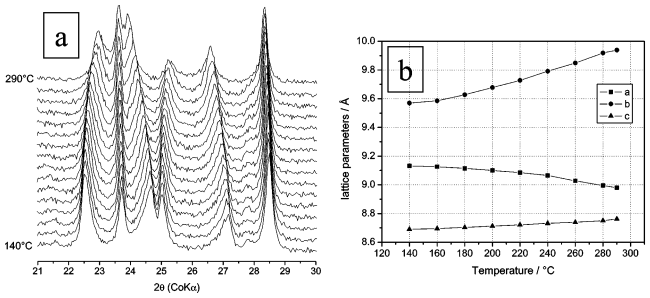

Figure 6. Structural evolution of $FePO_4$ III between 140 °C and 290 °C. Detail of the X-ray sequence during annealing (a) and plot of the lattice parameters evolution (b).

Song's data[13] (Table 4). $FePO_4$ III is stable between ∼140 and ∼300 °C, but we found, as clearly illustrated in Figure 6, that the orthorhombic lattice parameters vary anisotropically in this temperature range. When the temperature reaches approximately 310 °C the structure of orthorhombic $FePO_4$ III collapses and transforms to another allotrope of $FePO_4$ that adopts, this time, the so-called tridymite structure. The tridymite structure is, strictly speaking, the hexagonal ($P6_3/mmc$) high-temperature allotrope of SiO_2. It consists of corner-sharing tetrahedra organized as six member rings, constituting antiparallel layers stacked in the direction of the hexagonal *c* axis. The vertexes of the tetrahedra point alternatively up and down. In the literature, the phospho-tridymite usually refers to the hexagonal ($P6_3mc$) allotrope of $AlPO_4$.[28−29] In our case, the tetrahedra are alternatively occupied by Fe or P which reduces the space group symmetry from $P6_3/mmc$ to $P6_3mc$; all the diffraction peaks of $FePO_4$ at 320 °C are indexed in the $P6_3mc$ space group of the phospho-tridymite structure until ∼500 °C. Note that no structural data have been reported so far on the tridymite form of $FePO_4$. Ai prepared a so-called tridymite polymorph of $FePO_4$[30−31] by annealing amorphous $FePO_4{\cdot}nH_2O$ at 400 °C for 8 h and evaluated its catalytic activity in oxidative dehydrogenation reactions. At 450 °C, FePO4 III starts to convert into α-quartz $FePO_4$. At ∼520 °C, the transformation is completed and pure α-quartz $FePO_4$ is stable until 710 °C, at which the α → *β* conversion takes place.[32]

4.2 Metastrengite I. Metastrengite I $FePO_4{\cdot}2H_2O$ transforms to another variety of $FePO_4$ at 140 °C, labeled as $FePO_4$ I by Rémy,[21−22] and then to $FePO_4$ tridymite at a relatively moderate temperature (∼240 °C) (Figure 7, Table 3). The XRD pattern of $FePO_4$ I differs only slightly from that of the tridymite by the appearance of convoluted peaks at $2\theta \cong 31°$. These may

(28) Rokita, M.; Handke, M.; Mozgawa, W. *J. Mol. Struct.* **1998**, *450*, 213−217.
(29) Graetsch, H. A. *Acta Crystallogr.* **2001**, *C57*, 665−667.
(30) Ai, M.; Ohdan, K. *J. Mol. Catal. A: Chem.* **2000**, *159*, 19−24.
(31) Ai, M.; Ohdan,K. *Appl. Catal. A: Gen.* **1999**, *180*, 47−52.
(32) Philippot, E.; Goiffon, A.; Ibanez, A.; Pintard, M. *J. Solid State Chem.* **1994**, *110*, 356−362.

Table 4. Crystallographic Data of the Phases Obtained by Annealing of the Crystalline Iron Orthophosphates

	T/°C	space group	*a*/Å	*b*/Å	*c*/Å	*β*/°
strengite	30	*Pbca*	9.881(2)	10.115(2)	8.719(2)	
	120		9.894(2)	10.116(2)	8.741(2)	
$FePO_4$ III	140	*Pbca*	9.132(6)	9.569(6)	8.690(6)	
	290		8.980(8)	9.939(9)	8.762(7)	
tridymite	310	$P6_3mc$	5.204(9)	5.204(9)	8.516(9)	
	440		5.209(9)	5.209(9)	8.532(9)	
α-quartz	520	$P3_121$	5.103(7)	5.103(7)	11.333(7)	
	700		5.165(8)	5.165(8)	11.383(9)	
β-quartz	800	$P6_422$	5.175(8)	5.175(8)	11.392(9)	
metastrengite I	40	*Pbnm*	5.217(2)	10.032(6)	8.93(1)	
	130		5.217(2)	10.045(6)	8.92(1)	
$FePO_4$ I	160	$P2_1$	10.93(2)	5.46(1)	8.09(2)	122.74(5)
tridymite	260	$P6_3mc$	5.19(1)	5.19(1)	8.50(1)	
	520		5.192(8)	5.192(8)	8.523(8)	
α-quartz	620	$P3_121$	5.11(1)	5.11(1)	11.32(1)	
metastrengite II	30	$P2_1/n$	5.318(1)	9.785(2)	8.698(2)	90.52(2)
	130		5.321(1)	9.813(2)	8.719(2)	90.49(1)
$FePO_4$ II	140	$P2_1/n$	5.46(1)	7.51(1)	8.04(1)	95.7(1)
	550		5.471(2)	7.607(9)	8.120(9)	96.78(6)
α-quartz	640	$P3_121$	5.092(6)	5.092(6)	11.297(9)	

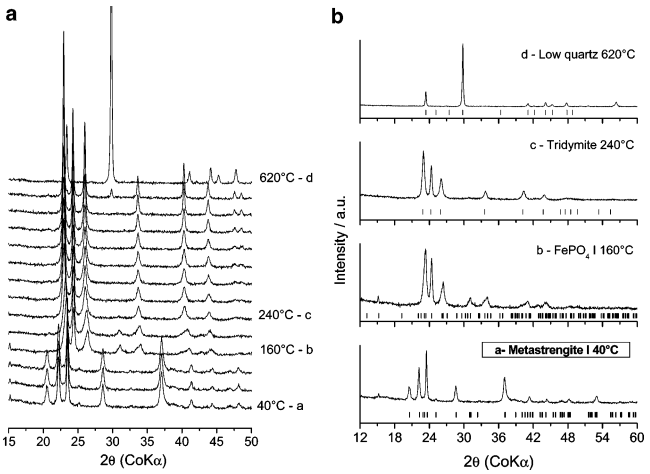

Figure 7. (a) XRD diffraction patterns evolution of $FePO_4 \cdot 2H_2O$ metastrengite I under thermal treatment. Measurement conditions are the same as those in Figure 5. (b) Details of the XRD pattern of the phases produced by annealing of metastrengite I; Co Kα radiation.

be indexed using a monoclinic cell in the space group $P2_1$ (Table 4), in good agreement with Graetsch's work on tridymite forms of $AlPO_4$.[33] This suggests that $FePO_4$ I might be a low-temperature modification of the phospho-tridymite high-temperature form. Indeed, this latter is not stable at RT and transforms reversibly into $FePO_4$ I upon cooling. Additionally, $FePO_4$ I turns out to be extremely sensitive to air moisture and rehydrates up to the final composition $FePO_4 \cdot \sim 1.4\ H_2O$, as shown by the weight uptake on a metastrengite I sample previously annealed at 400 °C (Figure 8c). These results corroborate Rémy's work, who reported a water up-take of $FePO_4$ I corresponding to 1.6 H_2O per $FePO_4$ after 1.5 years.[21] The annealing temperature of metastrengite I does not seem to have an influence upon the amount of water taken up. As an example, a sample annealed at 180 °C exhibits a water content of 1.3 H_2O per $FePO_4$ after re-hydration. In contrast, a diminishing of the crystallinity of the re-hydrated phase is observed as annealing temperature increases. Figure 8b shows the XRD pattern obtained for a sample annealed at 180 °C and re-hydrated under air moisture. A major difference

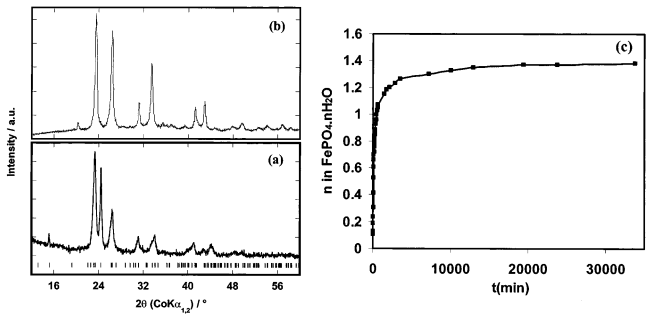

Figure 8. XRD diffraction patterns of $FePO_4$ I before (a) and after re-hydration under air moisture (b); Co Kα radiation. (c) Water uptake versus time of a sample previously annealed at 400 °C.

between XRD patterns of $FePO_4$ I and the re-hydrated form is the disappearance of the intense reflection at $2\theta = 24.4°$. Synchrotron X-ray diffraction experiments will be run in the near future to determine which structural rearrangements take place in this reaction. Formation of α-quartz $FePO_4$ starts to proceed from 540 °C, and the pure phase is obtained at ∼620 °C. Note that the α-quartz $FePO_4$ formation occurs at a higher temperature than that for strengite. With the nature of the transition being the same (tridymite $FePO_4 \rightarrow$ α-quartz $FePO_4$), the delay observed when heating metastrengite I should be due to kinetic limitations, but we do not understand exactly why.

4.3 Metastrengite II. The dehydration of the monoclinic form of $FePO_4 \cdot 2H_2O$ (metastrengite II) occurs as a simple series of phase transformations, as shown by Figure 9. Unlike the two other allotropes, $FePO_4$ tridymite does not form as an intermediate phase during the annealing sequence. At 140 °C, dehydration leads to an anhydrous monoclinic allotrope called $FePO_4$ II[21−22] that was recently investigated in detail by Song.[13] Upon departure of H_2O groups, the remaining Fe−O−P skeleton is basically unaffected, although iron becomes tetracoordinated (average Fe−O bond length = 1.87 Å[13]). This phase transformation corresponds to a shrinkage of about 27%, much higher than that occurring for orthorhombic strengite. This phase is stable until 550 °C at which α-quartz $FePO_4$ starts to form. At ∼650 °C, the transformation is completed. The α−*β* conversion occurs as previously at 710 °C.

(33) Graetsch, H. A. *Acta Crystallogr.* **2002**, *C58*, i18−i20.

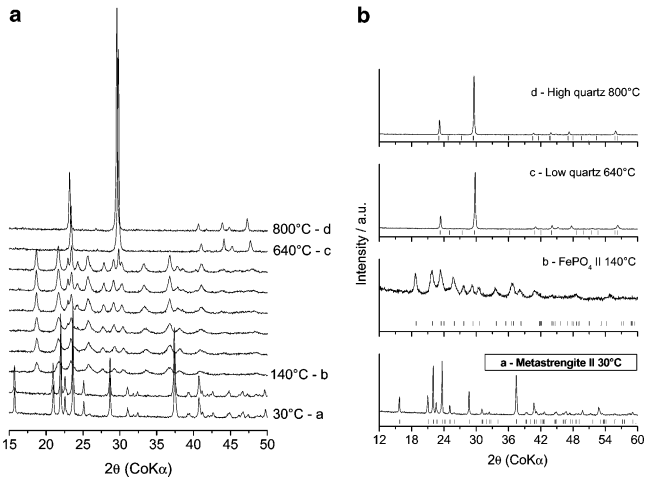

Figure 9. (a) XRD diffraction patterns evolution of $FePO_4 \cdot 2H_2O$ metastrengite II under thermal treatment. Measurement conditions are the same as those in Figure 5. (b) Details of the XRD pattern of the phases produced by annealing of metastrengite II; Co Kα radiation.

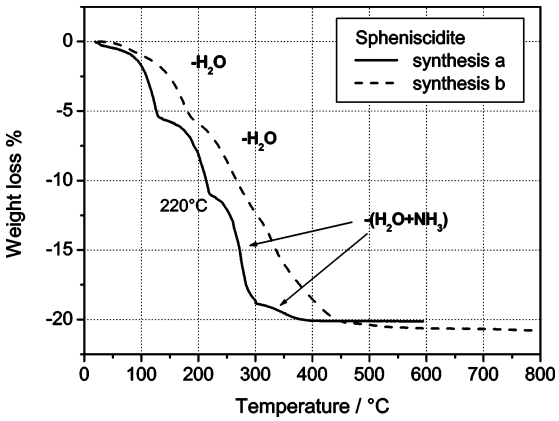

Figure 10. Thermogravimetric analysis of $NH_4(Fe_2(PO_4)_2OH \cdot H_2O) \cdot H_2O$. Heating rate: 1 °C/min from 25 to 300 °C and 5 °C/min from 300 to 800 °C.

4.4 Spheniscidite. Spheniscidite $NH_4(Fe_2(PO_4)_2OH \cdot H_2O) \cdot H_2O$ was found to evolve, ultimately, into $FePO_4$ quartz as well, but in a complex series of phase transformations. Figure 10 shows the thermogravimetric data recorded while heating two different samples of spheniscidite. The small particles of sample "a" (prepared at RT) lose globally 3 H_2O groups and 1 NH_3 group per $FePO_4$ in three well-defined steps. Higher temperatures and smoother steps are systematically observed for bigger particles of sample "b". A close examination of the structural arrangement of pristine spheniscidite beside temperature-controlled X-ray diffraction (Figure 11) and infrared transmission spectroscopy (Figure 12) allowed to account for this interesting thermogravimetric behavior.

As mentioned in Section 3.4, the formulation $[Fe_2(PO_4)_2(OH) \cdot (H_2O)] \cdot (NH_4) \cdot H_2O$ accounts for the existence in the spheniscidite structure of 1 H_2O molecule and 1 NH_4^+ ion that are not directly linked to iron atoms. The first weight loss until ~140 °C corresponds most likely to the departure of the "free" H_2O group without any significant structural rearrangement: the X-ray diffraction pattern of $[Fe_2(PO_4)_2(OH) \cdot (H_2O)] \cdot (NH_4)$ was indexed, as for pristine spheniscidite, in the space group $P2_1/n$ with $a = 9.65(1)$ Å, $b = 9.94(1)$ Å, $c = 9.72(1)$ Å,

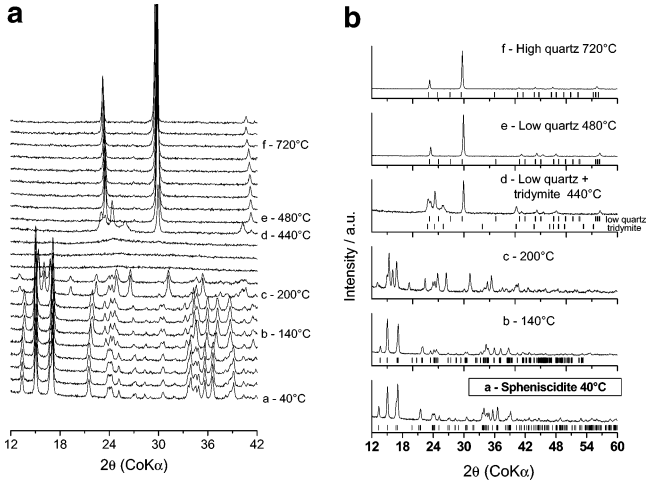

Figure 11. (a) In situ diffraction patterns evolution of $NH_4(Fe_2(PO_4)_2OH \cdot H_2O) \cdot H_2O$ with thermal treatment. Measurement conditions are the same as those in Figure 5. (b) Details of the XRD pattern of the phases produced; Co Kα radiation.

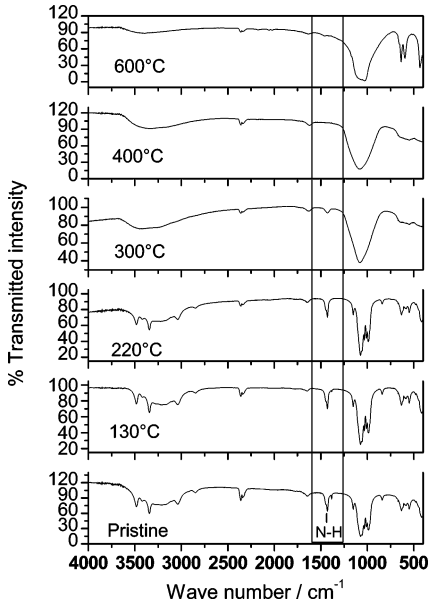

Figure 12. IR transmission spectra of a pristine $NH_4(Fe_2(PO_4)_2OH \cdot H_2O) \cdot H_2O$ sample and of powders annealed at 130, 220, 300, 400, and 600 °C and stored in air.

and $\beta = 102.39(3)°$, leading to a slight anisotropic shrinkage of almost 1%. Between 140 and 200 °C, a second well-defined step corresponds to the departure of the remaining (H_2O) group that leads to the crystalline form of $[Fe_2(PO_4)_2(OH)] \cdot (NH_4)$, never reported so far. Importantly, this is accounted for by the fact that the solid obtained at 200 °C, when re-exposed to air moisture at room temperature, transforms back to spheniscidite. The third process, between 220 °and ~300 °C, corresponds to the departure of NH_4^+ and OH^- (NH_3 and H_2O) and to the complete amorphization of the solid. From the structural description given in Section 3.4, it may be easily understood that the departure of the bridging hydroxyl group H−O(7) (connecting $Fe(2)O_6$ octahedra) results in a total collapsing of the structure. The progressive disappearance of the band at ~1400 cm^{-1} (ascribed to a bending mode of N−H bonds) on the IR spectra recorded for the samples annealed at $T > 220$ °C might be related to the departure of the ammonium ions. After this final decomposition,

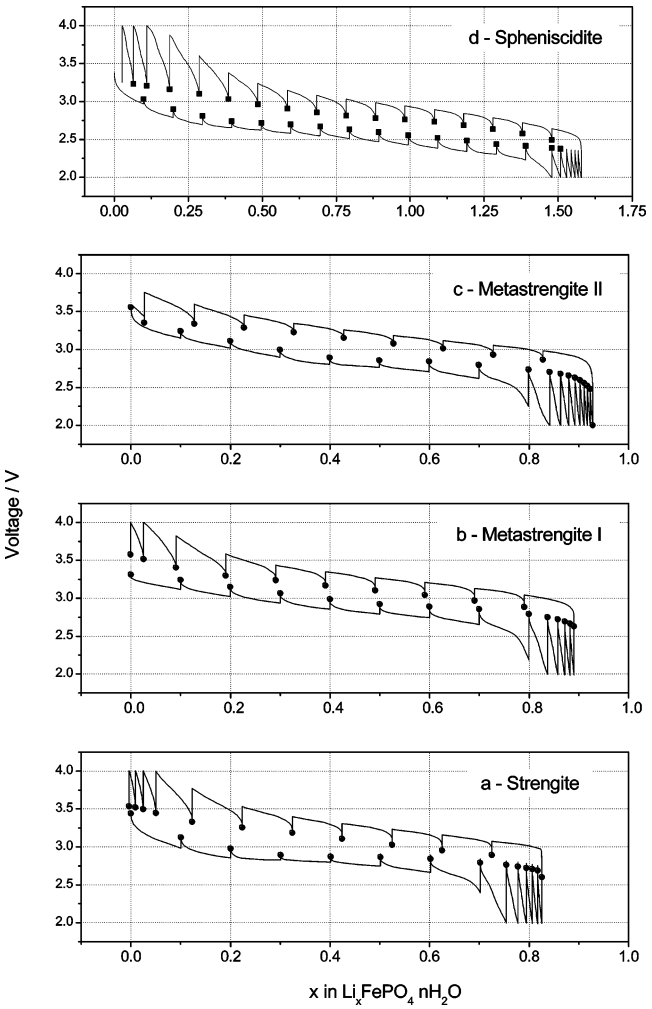

Figure 13. Galvanostatic intermittent titration curves of strengite (a), metastrengite I (b), metastrengite II (c), and spheniscidite (d) carbon composites. For each step, the current was set to a value corresponding to a C/10 rate for 1 h, followed by a relaxation period of 12 h.

the $FePO_4$ solid is amorphous and transforms finally to $FePO_4$ quartz via a temperature domain where a mixture of tridymite and α-quartz $FePO_4$ was observed.

5. Conclusion

Three pure $FePO_4 \cdot 2H_2O$ allotropes were synthesized by a precipitation technique in an aqueous medium, under pH and reaction-time control. The thermal treatment of these compounds allowed isolation and characterization of 6 $FePO_4$ allotropes, with iron in tetrahedral oxygen environment. Additionally, pure spheniscidite $NH_4(Fe_2(PO_4)_2OH \cdot H_2O) \cdot H_2O$ was obtained by a similar precipitation technique by using NH_3 to adjust pH.

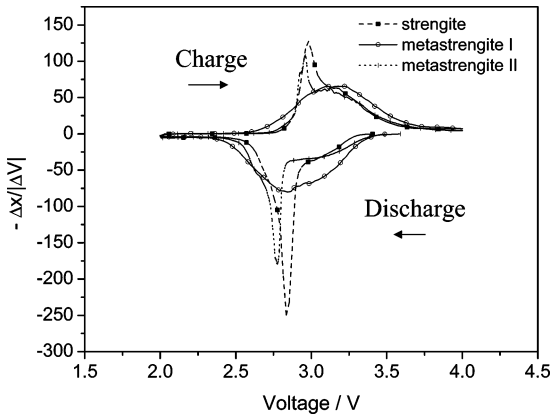

Figure 14. Derivative curves of the composition *x* versus potential.

All the hydrated crystalline powders synthesized were tested as positive electrode materials in lithium batteries. To this end, as described in detail elsewhere,[19] the powders were ball-milled for 90 min with acetylene black. Up to 0.8−0.9 lithium equivalents were inserted in the three crystalline $FePO_4 \cdot nH_2O$ allotropes (strengite, metastrengite I, and metastrengite II), within the 2−4 V vs Li^+/Li region (Figure 13). As for the amorphous $FePO_4 \cdot nH_2O$ powders that we investigated,[19] the presence of H_2O groups within the crystalline structures does not represent a drawback for reversible electrochemical activity on the Fe^{3+}/Fe^{2+} couple in this voltage domain. For strengite and metastrengite II, two-phase processes are clearly identified at a potential ∼2.8−2.9 V vs Li^+/Li on the derivatives curves $-\Delta x/|\Delta V|$ (Figure 14) whereas lithium insertion in metastrengite I occurs in a single-phase process. Concerning the spheniscidite $NH_4(Fe_2(PO_4)_2OH \cdot H_2O) \cdot H_2O$, 1.5 lithium equivalents (for 2 irons) could be inserted, reversibly as well, in a voltage window of 3.2−2.0 V vs Li^+/Li. Interestingly, the average voltage is lower than that for $FePO_4 \cdot nH_2O$, this being consistent with the existence of the Fe_4O_{20} clusters that diminish the overall inductive effect of the PO_4 groups on the Fe^{3+}/Fe^{2+} couple. Further experiments are in progress so as to elucidate more precisely the electrochemical mechanisms of each of these 4 hydrated powders, and those of the stable forms (at RT) of anhydrous $FePO_4$ isolated in this study. Indeed, one of the goals would be to elucidate the role of structural water in the hydrated forms.

Acknowledgment. We thank Dr. D. Larcher and Pr. J-M. Tarascon for fruitful and helpful scientific discussions.

CM031107Z